

The contribution of ancient admixture to reproductive isolation between European sea bass lineages

Short Title: *Ancient admixture in sea bass speciation*

Maud Duranton^{1*}, François Allal², Sophie Valière³, Olivier Bouchez³, François Bonhomme¹ and Pierre-Alexandre Gagnaire¹

¹ ISEM, Univ Montpellier, CNRS, EPHE, IRD, Montpellier, France

² MARBEC, Université de Montpellier, Ifremer-CNRS-IRD-UM, Palavas-les-Flots, France

³ INRA, US 1426, GeT-PlaGe, Genotoul, Castanet-Tolosan, France.

*Corresponding author

1 **Abstract:**

2

3 Understanding how new species arise through the progressive establishment of reproductive isolation
4 barriers between diverging populations is a major goal in Evolutionary Biology. One important result
5 of speciation genomics studies is that the genomic regions involved in reproductive isolation frequently
6 harbor anciently diverged haplotypes that predate the reconstructed history of species divergence.
7 The possible origins of these old alleles remain highly debated, since they relate to contrasted
8 mechanisms of speciation that are not fully understood yet. In the European sea bass (*Dicentrarchus*
9 *labrax*), the genomic regions involved in reproductive isolation between Atlantic and Mediterranean
10 lineages are enriched for anciently diverged alleles of unknown origin. Here, we used haplotype-
11 resolved whole-genome sequences to test whether divergent haplotypes could have originated from
12 a closely related species, the spotted sea bass (*Dicentrarchus punctatus*). We found that an ancient
13 admixture event between *D. labrax* and *D. punctatus* is responsible for the presence of shared derived
14 alleles that segregate at low frequencies in both lineages of *D. labrax*. An exception to this was found
15 within regions involved in reproductive isolation between the two *D. labrax* lineages. In those regions,
16 archaic tracts originating from *D. punctatus* locally reached high frequencies or even fixation in Atlantic
17 genomes but were almost absent in the Mediterranean. We showed that the ancient admixture event
18 most likely occurred between *D. punctatus* and the *D. labrax* Atlantic lineage, while Atlantic and
19 Mediterranean *D. labrax* lineages were experiencing allopatric isolation. Our results suggest that local
20 adaptive introgression and/or the resolution of genomic conflicts provoked by ancient admixture have
21 probably participated to the establishment of reproductive isolation between the two *D. labrax*
22 lineages.

23

24 **Author summary**

25 Speciation is often viewed as a progressive accumulation of reproductive isolation barriers between
26 two diverging lineages through the time. When initiated, the speciation process may however take
27 different routes, sometimes leading to the erosion of an established species barrier or to the
28 acquisition of new speciation genes transferred from another species boundary. Here, we describe
29 such a case in the European sea bass. This marine fish species has split 300,000 years ago into an
30 Atlantic and a Mediterranean lineage, which remained partially reproductively isolated after
31 experiencing postglacial secondary contact. For unknown reasons, genomic regions involved in
32 reproductive isolation between lineages have started to diverge well before the split. We here show
33 that diverged alleles were acquired by the Atlantic lineage from an ancient event of admixture with a
34 parapatric sister species about 80,000 years ago. Introgressed foreign alleles that were locally driven

35 to high frequencies in the Atlantic have subsequently resisted to introgression within the
36 Mediterranean during the postglacial secondary contact, thus contributing to increased reproductive
37 isolation between two sea bass lineages. These results support the view that reproductive isolation
38 barriers can evolve via reticulate gene flow across multiple species boundaries.

39

40

Introduction

41

42 Speciation is the evolutionary process that leads to the emergence of new species through the
43 progressive establishment of Reproductive Isolation (RI) barriers between diverging populations (1).
44 Identifying those barriers and understanding the eco-evolutionary context in which they evolved has
45 been at the core of the speciation genetics research program (2,3). Over the last decade, progresses
46 in sequencing technologies have allowed to gain important insights into the genetic basis of
47 reproductive isolation barriers through the study of genome-wide differentiation/divergence patterns
48 between closely related species (4–8). An important result of speciation genomics studies was that the
49 age of the alleles located within genomic regions involved in RI is often much older than the average
50 coalescent time computed across the whole genome. This finding indicates that the regions involved
51 in RI tend to be enriched for anciently diverged haplotypes. An example of this comes from the fixed
52 chromosomal inversions involved in RI between *Drosophila pseudoobscura* and *D. persimilis*, which
53 show higher divergence than collinear regions of the genome (9). Another case is provided by the large
54 genomic regions of ancient ancestry that have been found across the threespine stickleback's genome,
55 which are involved in RI between marine and freshwater populations (10,11). A third example, among
56 others (see [Marques *et al.* \(2019\)](#) for a review), was described in Darwin's finches, whereby genomic
57 regions showing increased divergence in several species pairs also display anciently diverged
58 haplogroups that originated before the species splits (13).

59 Different hypotheses can explain the origin and the maintenance of these highly divergent
60 haplotypes. First, polymorphism has possibly been maintained over the long term in the ancestral
61 population before being differentially sorted between the descendant lineages (14). This hypothesis
62 has been proposed to explain the excess of haplotype divergence in the aforementioned examples
63 (9,10,13). One mechanism that may explain the long-term maintenance of polymorphism is ancestral
64 population structure, that is, subdivision owing to barriers to gene flow in the ancestral population
65 (15). In addition to demography, balancing selection due to either frequency-dependent selection,
66 heterozygote advantage (overdominance) or heterogeneous selection in space or time (16) can also

67 promote the maintenance of ancient polymorphisms. For instance, in Darwin's finches, balancing
68 selection has been proposed to explain the maintenance of divergent haplogroups associated with
69 beak shape, due to the selective advantage of rare beak morphologies, or changing environmental
70 conditions inducing heterogeneous selection (13). An alternative explanation to the presence of
71 anciently diverged alleles is admixture with a divergent lineage. Contemporary hybridization has long
72 been recognized as a common phenomenon in plants and animals (17,18), and cases of ancient
73 admixture are increasingly detected by genomic studies. One emblematic example is past admixture
74 between modern humans and two extinct archaic hominin lineages, Neanderthal and Denisova (19–
75 21). More recently, ancient introgression from the extinct cave bear has also been detected in the
76 genomes of living brown bears (22). Therefore, past admixture is increasingly recognized as a source
77 of anciently diverged alleles in contemporary genomes.

78 Understanding why and how divergent haplogroups tend to disproportionately contribute to
79 the buildup of RI between nascent species remains, however, highly challenging. First, because
80 retention of ancestral polymorphism and past admixture are notoriously difficult to distinguish and
81 not mutually exclusive hypotheses to explain the presence of anciently diverged alleles (23–27).
82 Furthermore, identifying the genomic regions that resist introgression is still a major obstacle to the
83 detection of RI loci (28). These tasks are now facilitated by the direct assessment of local ancestry along
84 individual genome sequences (29,30), thus paving the way for assessing the role of ancient admixture
85 in speciation. Here, we use new haplotype-resolved whole-genome sequences to delineate the regions
86 involved in RI between European sea bass lineages and understand the origin of the divergent
87 haplogroups they contain.

88 The European sea bass (*Dicentrarchus labrax*) is a marine fish subdivided into two glacial
89 lineages, which currently correspond to Atlantic and Mediterranean populations (31). These two
90 lineages have diverged in allopatry for *c.a.* 300,000 years before experiencing a secondary contact
91 since the last glacial retreat (32). Postglacial gene flow between the two lineages is strongly
92 asymmetrical, mostly occurring from the Atlantic to the Mediterranean genetic background (32). This
93 resulted in a spatial introgression gradient within the Mediterranean Sea, illustrated by a more than
94 twofold higher Atlantic ancestry in the western (31%) compared to the eastern (13%) Mediterranean
95 population (30). A detailed analysis of local ancestry tracts across Mediterranean and Atlantic sea bass
96 genomes has provided direct evidence for highly heterogeneous rates of gene flow along most
97 chromosomes (Duranton *et al.* 2018). This mosaic introgression pattern was attributed to the effect of
98 multiple small effect RI loci mainly located in low-recombining regions that present particularly high
99 values of nucleotidic divergence (d_{XY}). It is generally assumed that increased d_{XY} indicates the presence
100 of haplotypes that started to diverge earlier than the rest of the genome. However, regions of

101 increased divergence may simply have resisted gene flow during secondary contact, while haplotypes
102 in the remainder of the genome got rejuvenated due to recombination. This later hypothesis, however
103 has been rejected in the European sea bass using simulations accounting for both background selection
104 and selection against introgressed tracts (30). Therefore, anciently diverged alleles are unlikely to have
105 evolved within the 300,000 years divergence history inferred from genome-wide polymorphism data
106 and are thus older. In the present study, we use new haplotype-resolved whole-genome sequences to
107 accurately delineate regions involved in RI and investigate the mechanisms underlying their excess of
108 divergence. We specifically test for past admixture with a closely related species using a new genome
109 sequence from the parapatrically distributed spotted sea bass (*Dicentrarchus punctatus*). Our results
110 show that gene flow occurred between *D. punctatus* and the Atlantic lineage of *D. labrax* about 80,000
111 years ago, resulting in a low background ancestry from *D. punctatus* in contemporary *D. labrax*
112 genomes. By contrast, genomic regions involved in RI between the two *D. labrax* lineages generally
113 display high frequencies of haplotypes derived from *D. punctatus* in the Atlantic, while these archaic
114 tracts remain rare in the Mediterranean. This suggests that ancient admixture has played an important
115 role in the evolution of RI between Atlantic and Mediterranean sea bass lineages, consistently with
116 predictions from models of local adaptive introgression and selection against genetic incompatibilities.

117 **Results**

118 ***Phylogenomic analysis***

119 We reconstructed the genetic relationships among the three Moronid species used in our study: the
120 striped bass (*Morone saxatilis*), the spotted sea bass (*Dicentrarchus punctatus*) and the European sea
121 bass (*Dicentrarchus labrax*), which is further subdivided into two partially reproductively isolated
122 populations: the Atlantic and Mediterranean sea bass lineages. All of the 3,329 maximum-likelihood
123 phylogenetic trees generated in non-overlapping 50kb windows showed the same topology,
124 corresponding to the expected species tree (Figure 1A). However, when similar reconstructions were
125 performed in 2 kb windows, 4.6% of conflicting genealogies were found with an excess of trees in
126 which *D. punctatus* grouped with the Atlantic (2.87%) versus with the Mediterranean (1.68%) *D. labrax*
127 lineage (Supplementary Figure 3). The relative branch lengths of the species tree largely reflected the
128 mean nucleotide divergence (d_{xy}) measured between each pair of four species/lineages (Figure 1B).
129 We found 4.5% of absolute sequence divergence between the outgroup *M. saxatilis* and the two
130 *Dicentrarchus* species. Divergence between *D. labrax* and *D. punctatus* (0.55%) was more than five
131 times higher than divergence between Atlantic and Mediterranean *D. labrax* lineages (0.1%),
132 consistently with previous estimates (30,32). We found a slightly higher divergence between *D.*
133 *punctatus* and the eastern Mediterranean (0.56%) compared to the Atlantic *D. labrax* lineage (0.53%).

134 Within *D. labrax*, divergence to the Atlantic population was higher for the eastern (0.1%) compared to
135 the western Mediterranean population (0.09%) (consistent with the PCA, Supplementary Figure 2), as
136 expected due to gene flow between Atlantic and Mediterranean *D. labrax* lineages (30,32).

137

138 **Test for foreign introgression within *D. labrax***

139 Chromosomal patterns of absolute sequence divergence (d_{XY}) between the Atlantic and Mediterranean
140 lineages of *D. labrax* (Fig 2A and Supplementary Figure 4A) showed highly heterogeneous divergence
141 along the genome, as reported in previous studies (30,32). To determine if local excesses of d_{XY} can be
142 explained by past admixture with another lineage, we first looked for gene flow between *D. labrax*
143 lineages and *D. punctatus* using the ABBA-BABA test. Some genomic regions showed particularly high
144 values of the f_D statistics, thus reflecting locally elevated ancestry from *D. punctatus* within the *D.*
145 *labrax* Atlantic lineage (Figure 2B and Supplementary Figure 4B red curve). By contrast, when the f_D
146 statistics was used to measure local *D. punctatus* ancestry within *D. labrax* Mediterranean populations,
147 low and relatively homogeneous introgression patterns were found across the entire genome (Figure
148 2B and Supplementary Figure 4B blue and green curves). This finding thus indicates highly
149 heterogeneous introgression of spotted sea bass alleles within the Atlantic *D. labrax* lineage, and
150 comparatively lower introgression within the Mediterranean lineage.

151 We also searched for the presence of archaic introgressed tracts in *D. labrax* genomes. A
152 relatively low fraction of archaic tracts (F_{archaic}) was found along the genome in both Atlantic (4.85% in
153 non-RI islands) and Mediterranean (2.73% in non-RI islands) *D. labrax* individuals (Figure 2C and
154 Supplementary Figure 4C). In some regions, however, F_{archaic} was particularly high in the Atlantic (i.e.
155 >30%) compared to the Mediterranean lineage. Interestingly, those regions also presented the highest
156 f_D values (Figure 2B red curve), and there was a highly significant positive correlation between f_D and
157 F_{archaic} in Atlantic *D. labrax* genomes (Spearman's rho = 0.281***). These results thus support the
158 hypothesis that the detected archaic segments that locally reach high frequencies in some regions of
159 Atlantic *D. labrax* genomes have been inherited from *D. punctatus* at some time in the past.
160 Furthermore, regions of particularly increased *D. punctatus* ancestry also showed the highest absolute
161 divergence values between Atlantic and Mediterranean *D. labrax* lineages, with positive genome-wide
162 correlations being found with d_{XY} for both f_D (Spearman's rho = 0.281***) and F_{archaic} (Spearman's rho
163 = 0.531***). Lastly, we used the RND_{min} statistics to detect chromosomal variations in ancient
164 introgression. Values of RND_{min} measured between *D. punctatus* and the Atlantic *D. labrax* lineage
165 were low and relatively constant along chromosomes (Figure 2D and 4D red curves), indicating
166 widespread (although locally rare) introgression across the genome. By contrast, RND_{min} was higher

167 and highly variable when measured with the Mediterranean *D. labrax* populations (Figure 2D and 4D
168 blue and green curves), indicating that introgression from *D. punctatus* is absent or nearly absent in
169 some genomic regions of the Mediterranean lineage. These regions, that seem resistant to *D.*
170 *punctatus* introgression in Mediterranean *D. labrax* genomes, also showed elevated values of F_{archaic}
171 (genome-wide Spearman's rho = 0.472***) and f_D (genome wide spearman's rho = 0.223***) in
172 Atlantic genomes, along with increased d_{XY} between Atlantic and Mediterranean *D. labrax* lineages
173 (genome-wide Spearman's rho = 0.717***). These results thus indicate the existence of outlying
174 patterns of *D. punctatus* ancestry in the most divergent genomic regions between *D. labrax* lineages,
175 due to respectively increased and decreased frequencies of anciently introgressed tracts in the Atlantic
176 and Mediterranean lineages, compared to the background level.

177 Finally, our HMM approach allowed categorizing 70,738 SNP that are likely associated with RI
178 islands between the two *D. labrax* lineages (Figure 2E and Supplementary Figure 4E). We found a good
179 concordance between the positions of RI islands identified with the SNP and window-based methods,
180 although the former allowed us to detect narrower RI-associated regions with a higher resolution
181 (Supplementary Figure 5C and F). As expected, all these regions displayed increased levels of ancient
182 *D. punctatus* introgression in the Atlantic but decreased *D. punctatus* ancestry in the Mediterranean
183 (Figure 2), thus strengthening the association of RI-islands to differential rates of archaic ancestry.

184

185 **Estimation of the time since introgression between *D. punctatus* and *D. labrax***

186 We estimated the timing of past gene flow between *D. punctatus* and *D. labrax* by first comparing the
187 length distribution of *D. punctatus* tracts introgressed into Atlantic *D. labrax* genomes to that of
188 Atlantic *D. labrax* tracts introgressed into western Mediterranean *D. labrax* genomes (Figure 3A). The
189 two distributions showed similar shapes although *D. punctatus* tracts were on average almost ten-time
190 shorter ($\bar{L}_{\text{punctatus}} = 5,513$ kb) than Atlantic *D. labrax* tracts ($\bar{L}_{\text{labrax}} = 52,026$ kb). *D. punctatus* tracts were
191 also less abundant in almost all length classes except for the shortest tracts (Figure 3A). We estimated

192 the average time since introgression for both distributions as $t_{\text{labrax-punctatus}} = \frac{1}{((1 - 0.096) \cdot 3.693e^{-8} \cdot 5513)}$

193 + 1 and $t_{\text{Atlantic-Mediterranean}} = \frac{1}{((1 - 0.341) \cdot 3.23e^{-8} \cdot 52026)} + 1$, which placed the contact between *D.*

194 *punctatus* and *D. labrax* approximately 6 times earlier than the one between the two *D. labrax*
195 lineages. Using the age of secondary contact previously estimated between Atlantic and
196 Mediterranean sea bass lineages (i.e. 11,500 years, Tine et al. 2014; Duranton et al. 2018) as a
197 calibration time-point, ancient gene flow between the two species was dated to ca. 70,000 years ago.
198 Secondly, we converted the estimated values of the transition parameter (p) of the HMM model used
199 to detect archaic introgressed tracts to estimate one value of T_{admix} for each chromosome

200 (Supplementary Table 2). From the obtained time distribution (Figure 3B), we estimated the most
201 probable time of ancient admixture to $T_{\text{admix}} = 91,149$ (CI_{90%} = [85,831 ; 110,645]) years.

202

203 ***The frequency of D. punctatus derived mutations in D. labrax***

204 We used the conditioned site frequency spectrum between Atlantic and Mediterranean lineages as a
205 way to represent how derived *D. punctatus* alleles segregate in *D. labrax*. For SNPs that were not
206 associated to RI-islands by the HMM approach, the one-dimensional distribution of allele frequencies
207 (CSFS) was highly similar between Atlantic and Mediterranean *D. labrax* lineages, showing a bimodal
208 shape with few intermediate frequency variants (Figure 4A). Most *D. punctatus* derived alleles were
209 present at either low or high frequencies, with ancestral mutations almost fixed in both *D. labrax*
210 lineages being about 100 times more abundant than *D. punctatus* derived mutations almost fixed in
211 both *D. labrax* lineages in the CSFS (Figure 4C). This result showed that the combined effects of
212 incomplete lineage sorting and introgression during species divergence has resulted in very similar
213 amounts of *D. punctatus* derived mutations between Atlantic and Mediterranean *D. labrax* lineages.
214 By contrast, SNPs found to be associated with RI islands showed a large excess of *D. punctatus* derived
215 alleles that were fixed or almost fixed in the Atlantic population, while segregating at low frequencies
216 in the Mediterranean populations (Figure 4B and D). This remained true whatever the Mediterranean
217 population (east, west or both) considered in the analysis (Supplementary Figure 7). The excess of high-
218 frequency *D. punctatus* derived mutations in the Atlantic sea bass lineage was also clearly visible in the
219 reversal of the CSFS in RI islands compared to non-RI regions (Figure 4A and B). Therefore, differential
220 introgression of *D. punctatus* derived mutations in RI islands is most likely due to their direct role in
221 reproductive isolation, rather than a delayed post-glacial rehomogenization due to already-existing
222 genetic barriers between *D. labrax* lineages in these regions.

223

224

224 **Discussion**

225

226 Recent speciation genomics studies have revealed that genomic regions involved in RI often contain
227 anciently diverged alleles (e.g. [Meier et al. 2017](#); [Han et al. 2017](#); [Nelson and Cresko 2018](#)). One of the
228 competing hypotheses to explain their origin is ancient admixture with an already diverged lineage.
229 Our main objective here was to determine if such a scenario could explain the excess of divergence
230 observed in RI regions between Atlantic and Mediterranean *D. labrax* lineages (30). To achieve this
231 goal, we used different complementary approaches that collectively provided strong support for
232 ancient introgression from the sister species *Dicentrarchus punctatus*. Despite low divergence ($d_{xy} =$

233 0.55%), partially overlapping range distributions and interfertility in artificial crosses (48),
234 contemporary hybridization has not been observed in the wild between *D. labrax* and *D. punctatus*
235 (Tine et al. 2014). We here show that interspecies admixture has likely happened earlier in the past,
236 bringing new key elements to understand the complex evolutionary history of unachieved speciation
237 between Atlantic and Mediterranean sea bass lineages.

238

239 **Extent of ancient admixture**

240 Overall, the average fraction of contemporary genomes derived from ancient admixture was lower
241 than 6% (i.e. 5.39% in the Atlantic and 2.82% in the Mediterranean lineage), which is only slightly higher
242 than the estimated persistence of archaic ancestry in humans and brown bears (22,49). Whether these
243 low background levels reflect a relatively limited contribution of genetic material from *D. punctatus*
244 during admixture, or the impact of long-term selection against admixed foreign ancestry (29,50,51)
245 was out of the scope of this study. Instead, we focused on understanding the marked excess of shared
246 derived mutations found between *D. punctatus* and the Atlantic compared to the Mediterranean *D.*
247 *labrax* lineage in RI-associated regions. This finding was strengthened by the locally increased
248 frequency of archaic introgressed tracts found in Atlantic genomes within regions associated to RI with
249 the Mediterranean lineage. Such locally elevated differences in the frequency of *D. punctatus* derived
250 alleles explain the increased sequence divergence previously observed in RI islands between Atlantic
251 and Mediterranean lineages (Duranton et al. 2018). Below, we consider potential limitations to the
252 detection of archaic introgression from contemporary genomes, and the related challenge of dating
253 ancient admixture. We then discuss how the genomic mosaicism of species ancestry may relate to
254 different mechanisms potentially involved in European sea bass speciation.

255

256 **Separating ancient introgression from shared ancestral variation**

257 Distinguishing past introgression and shared ancestral variation from ABBA-BABA and f_D statistics can
258 be difficult, especially in regions of reduced divergence (39). Therefore, the positive correlations
259 observed between f_D , the inferred frequency of archaic segments, and d_{XY} provided good support that
260 regions of high *D. punctatus* ancestry in the Atlantic are responsible for increased divergence between
261 *D. labrax* lineages. Admittedly, past gene flow may also have occurred with another now extinct
262 species rather than with *D. punctatus*, as it has been shown for other species (20,22,52). However,
263 since *D. labrax* harbors shared derived alleles with *D. punctatus*, any alternative ghost donor lineage
264 must have shared a long common history with the spotted sea bass.

265 Another potential issue with the tests performed to detect ancient admixture is that they often
266 rely on differential introgression patterns between two candidate recipient populations (39,40).
267 Therefore, these tests only enabled us to detect regions where the level of archaic introgression differs

268 between Atlantic and Mediterranean *D. labrax* lineages. This problem could be particularly acute
269 outside RI regions, where post-glacial gene flow between *D. labrax* lineages has almost completely
270 rehomogenized allele frequencies (Tine et al. 2014; Duranton et al. 2018). To determine whether *D.*
271 *punctatus* ancestry was simply absent or present but at similar levels in both lineages, we used the
272 RND_{min} statistics that does not rely on the comparison of two populations (Rosenzweig et al. 2016).
273 Low and nearly constant RND_{min} values indicated a widespread presence (although most of the time at
274 low frequencies) of anciently introgressed tracts along Atlantic *D. labrax* genomes. By contrast, regions
275 of elevated RND_{min} that coincided with the location of RI-islands revealed local resistance to
276 introgression in Mediterranean *D. labrax* genomes. Therefore, both lineages contain *D. punctatus*
277 introgressed tracts at relatively similar levels outside RI islands, which contrasts with strong archaic
278 ancestry differences found within RI-islands.

279

280 **Timing of ancient introgression**

281 To understand why *D. punctatus* alleles were rare within RI genomic regions in the Mediterranean, we
282 reconstructed the history of ancient admixture by estimating the time of contact between *D. punctatus*
283 and *D. labrax*. The two different methods respectively inferred a contact taking place approximately
284 70,000 and 90,000 years ago. Although these two estimates slightly differ, they both place ancient
285 admixture during the last glacial period (53), when Atlantic and Mediterranean *D. labrax* lineages were
286 inferred to be geographically isolated (30,32). The current distribution range of *D. punctatus* partially
287 overlaps with the southern part of the *D. labrax* distributional area in both the Atlantic (i.e. from
288 southern Biscay to Morocco) and southern Mediterranean Sea (i.e. North African shores). It is thus
289 likely that the latitudinal range shifts that occurred during quaternary ice ages (54) have favored
290 hybridization by further increasing the range overlap between the two species, as they were coexisting
291 in the Iberian or the north-western African Atlantic refugium (55). Once the two *D. labrax* lineages
292 came into secondary contact after the last glacial maximum, the *D. punctatus* alleles already
293 introgressed within Atlantic genomes could have readily introgressed Mediterranean genomes. This
294 hypothesis was supported by the observed gradient of decreasing *D. punctatus* ancestry from the
295 Atlantic to the eastern Mediterranean lineage, which mirrored the gradient in Atlantic ancestry
296 generated by the post-glacial secondary contact (30). The fact that *D. punctatus* tracts have most
297 probably introgressed the Mediterranean lineage secondarily, indicates that ancient hybridization has
298 only occurred in the Atlantic during the last glacial period. A possible explanation is the absence of
299 sympatry between *D. punctatus* and *D. labrax* within the Mediterranean during the last glacial period.
300 A missing piece of the reconstructed historical scenario remains with respect to the role of *D. punctatus*
301 alleles in RI.

302

303 **Causative role of high-frequency *D. punctatus* alleles in RI-islands**

304 If most of the currently observed RI-islands between *D. labrax* lineages were already existing before
305 ancient admixture with *D. punctatus*, such genetic barriers would have impeded the introgression of
306 *D. punctatus* alleles within the Mediterranean lineage (30). However, they would not account for
307 increased frequencies of *D. punctatus* derived alleles within RI-islands in the Atlantic lineage. The fact
308 that, in Atlantic *D. labrax*, regions associated to RI exhibited closely fixed *D. punctatus* derived alleles
309 that comparatively occurred at low frequencies elsewhere in the genome strongly supports their direct
310 role in the establishment of RI. This finding thus indicates that *D. punctatus* alleles have been first
311 locally driven to high frequencies in the Atlantic *D. labrax* lineage, while being secondarily prevented
312 from introgression within the Mediterranean lineage.

313

314

315

316 **Why anciently introgressed alleles contribute to RI?**

317 *Locally adaptive introgression*

318 Understanding the underlying evolutionary mechanisms through which admixture has contributed to
319 the buildup of reproductive isolation remains highly challenging (56,57). One evolutionary force that
320 can drive an allele to fixation is local positive selection. *D. punctatus* alleles may have fixed in the
321 Atlantic *D. labrax* lineage following admixture because they provided a selective advantage in the
322 Atlantic environment compared to ancestral *D. labrax* alleles, a process called adaptive introgression
323 (58). Several studies have revealed that the acquisition of adaptive phenotypes can be done through
324 hybridization, such as altitude adaptation in humans (59), mimicry in *Heliconius* butterflies (60) or
325 among others, seasonal camouflage in the snowshoe hares (61). Indeed, adaptive introgression allows
326 the rapid transfer of linked variants that have already been tested by natural selection in their original
327 environment, thus facilitating local adaptation (62). Therefore, it is theoretically possible that the
328 Atlantic *D. labrax* lineage has received from *D. punctatus* advantageous alleles in the Atlantic
329 environment that revealed to be deleterious in the Mediterranean Sea. Nevertheless, adaptive
330 introgression is usually difficult to prove since it can be confounded with other processes such as
331 uncoupling of an incompatibility from a multilocus genetic barrier (Fraïsse *et al.* 2014). Furthermore,
332 it has been argued that adaptive introgression cannot play an important role in reproductive isolation,
333 because unconditionally favorable alleles spread easily between diverging lineages until RI is nearly
334 complete (65).

335

336 *Fixation-compensation of deleterious mutations*

337 Another evolutionary force that may have driven *D. punctatus* derived alleles to fixation is genetic drift,
338 which can induce the fixation of deleterious mutations and thus increase mutation load (66). When
339 gene flow occurred between *D. punctatus* and *D. labrax* during the last glacial period, populations of
340 each species were probably experiencing bottlenecks (54), which decreased the efficiency of selection
341 and enhanced the probability to fix deleterious mutations by drift. Weakly deleterious *D. punctatus*
342 alleles may therefore have introgressed and fixed within the *D. labrax* Atlantic population. Another
343 related mechanism that may have influenced the outcome of hybridization is associative
344 overdominance, due to the masking of recessive deleterious mutations in admixed genotypes
345 (Whitlock et al. 2000; Bierne *et al.* 2002). Heterosis can locally increase the introgression rate of foreign
346 alleles, even if interbreeding populations have similar amounts of deleterious variation (68). Therefore,
347 heterosis may have favored the introgression of weakly deleterious *D. punctatus* variants in a
348 bottlenecked Atlantic *D. labrax* lineage. Subsequently, when Atlantic and Mediterranean *D. labrax*
349 lineages reconnected following postglacial recolonizations, expanding populations would have been
350 sufficiently large to reveal the deleterious effects of the introgressed alleles, generating hybrid
351 depression and hybridization load (29,69). Furthermore, the Atlantic population may have had enough
352 time to evolve compensatory mutations (70), which could have become substrate for increased RI. The
353 fact that most genomic regions involved in RI between *D. labrax* lineages exhibit low recombination
354 rates (Tine *et al.* 2014; Duranton et al. 2018) could indicate a role of slightly deleterious alleles in RI,
355 since selection is less efficient when linkage is strong.

356

357 *Reciprocal sorting of DMIs*

358 Reproductive isolation may also have evolved through the resolution of genetic conflicts resulting from
359 the contact between two diverged populations (71,72). Because each population has almost inevitably
360 fixed new adaptive or nearly neutral variants that reveal incompatible when combined in hybrid
361 genomes (73), Bateson-Dobzhansky-Muller incompatibilities (BDMIs) are recognized as a common
362 substrate for speciation (2). A genomic conflict induced by a two-locus BDMI can be resolved by fixing
363 one of either parental alleles. In a hybrid population generated by an equal mixture of individuals from
364 both parental populations, there is a 50% chance of fixing either parental combination (71). Therefore,
365 the resolution of multiple BDMIs in an admixed population offers ample opportunity to reciprocally
366 resolve independent BDMIs with respect to the origin of the parental allelic combination, which results
367 in RI from both parental populations. Even in the presence of skewed initial admixture proportions,
368 fixation of the minor parent combination can still happen with a sufficient number of BDMIs (71).
369 Therefore, the resolution of genetic conflicts between *D. punctatus* and *D. labrax* alleles in the Atlantic
370 lineage may have induced the fixation of *D. punctatus* alleles at some incompatibility loci. Upon contact
371 between Atlantic and Mediterranean *D. labrax* lineages, fixed *D. punctatus* alleles may have recreated

372 the BDMIs, thus contributing to RI. This non-adaptive speciation model due to selection against genetic
373 incompatibilities has the advantage to explain both the fixation of *D. punctatus* alleles within the *D.*
374 *labrax* Atlantic population, and their incompatibility with the Mediterranean lineage. Verbally, it can
375 be seen as a case whereby speciation reversal between lineages A and B contributes to strengthen RI
376 between lineages B and C through the transfer of incompatibilities between two porous species
377 boundaries.

378

379 **Conclusion**

380 To conclude, our results show that divergent haplotypes that were introgressed from *D. punctatus*
381 about 80,000 year ago have contributed to the strengthening of nascent RI between Atlantic and
382 Mediterranean *D. labrax* lineages. The resulting genomic architecture of RI between contemporary *D.*
383 *labrax* lineages is thus constituted by a mosaic of fixed blocks of different ancestries, that is, a mixture
384 of genetic barriers inherited from the own *D. labrax* divergence history and the contribution of ancient
385 admixture. Although additional analyses will be needed to fully understand which process has driven
386 the fixation of *D. punctatus* alleles within Atlantic genomes, the resolution of genetic conflicts between
387 *D. punctatus* and *D. labrax* seems the most parsimonious hypothesis (Schumer *et al.* 2015; Blanckaert
388 and Bank 2018). This speciation mechanism can be thought of as a transfer of incompatibilities
389 between two species boundaries, from the strongest to the weakest barrier, which is eventually
390 strengthened by the displacement of genetic conflicts inherited from an ancient episode of admixture.
391 Our finding adds to previous reports showing that postglacial and recent hybridization events have
392 played a role in the buildup of RI between admixed and parental lineages by generating similar genomic
393 mosaics of ancestries (29,74,75). The contribution of ancient admixture in European sea bass
394 speciation suggests that significantly older admixture events, which may have left cryptic signatures in
395 contemporary genomes, can be involved in seemingly recent speciation histories.

396

397

398 **Material and methods**

399

400 ***Whole-genome resequencing and haplotyping***

401 We sequenced the whole genome of one *Dicentrarchus punctatus* individual from the Atlantic Ocean
402 (Gulf of Cadiz, PUN) and 59 new *Dicentrarchus labrax* individual genomes. Fifty-two of them were wild
403 individuals captured from the Atlantic Ocean (English Channel, 10 males σ_{AT}), the western
404 Mediterranean Sea (Gulf of Lion, 14 females ♀_{WME} and 9 males σ_{WME}) and the eastern Mediterranean
405 Sea (Turkey, 10 males σ_{NEM} and Egypt, 9 males σ_{SEM}). Some of these specimens were involved in

406 experimental crosses to generate first generation hybrids. Seven F1 hybrids obtained from 7 different
407 biparental families (pedigree $\sigma_{ATX} \times \varphi_{WME}$) were also submitted to whole-genome sequencing. All captive
408 breeding procedures were performed at Ifremer's experimental aquaculture facility (agreement for
409 experiments with animals: C 34-192-6), where fish were reared in normal aquaculture conditions in
410 agreement with the French decree no. 2013-118 (1 February 2013 NOR:AGRG1231951D).

411 Whole genome sequencing libraries were prepared separately for each individual using either
412 the Illumina TruSeq DNA PCR-Free (40 individuals) or the TruSeq DNA Nano protocol (20 individuals),
413 depending on DNA concentration (Supplementary Table 1). Pools of 5 individually barcoded libraries
414 were then sequenced on 12 separate lanes of an Illumina HiSeq3000 using 2x150bp PE reads at the
415 GeT-PlaGe Genomics platform (Toulouse, France). Thirty-three individuals were sequenced twice due
416 to insufficient amounts of sequence reads obtained in the first run (Supplementary Table 1). For each
417 individual, the alignment of PE reads to the sea bass reference genome (32) was performed using BWA-
418 mem v0.7.5a (33) with default parameters. Duplicate reads were marked using Picard version 1.112
419 before being removed, producing a mean coverage depth of 33.8X per individual (Supplementary
420 Figure 1). We then followed GATK's (version 3.3-0-g37228af) best practice pipeline for individual
421 variant calling (using HaplotypeCaller), to joint genotyping, genotype refinement and variant filtering
422 (using Filter Expression: QD<10; MQ<50; FS>7; MQRankSum<-1.5; ReadPosRankSum<-1.5). We used
423 the BQSR algorithm to recalibrate base quality scores using a set of high-quality variants identified in
424 a previous study (30), and to perform variant quality score recalibration using the VQSR algorithm.
425 Hard filtering was then applied to exclude low-quality genotypes with a GQ score < 30. For the 7
426 mother-father-offspring trios, we used family-based priors for genotype refinement. We obtained a
427 total of 14,579,961 SNPs after filtering for indels, missing data (using --max-missing-count 8) and
428 removing the mitochondrial and ungrouped scaffolds (chromosome UN) in VCFtools v0.1.11 (34).

429 We performed haplotype phasing in *D. labrax* after removing the *D. punctatus* individual and
430 merging the 59 newly sequenced genomes with the 16 genomes already obtained in Duranton *et al.*
431 (2018). Fifteen individuals that were involved in family crosses (i.e. newly sequenced or not already
432 phased in the previous study) were submitted to phasing-by-transmission using the
433 PhaseByTransmission algorithm in GATK with default parameters and a mutation rate prior of 10^{-8} for
434 *de novo* mutations. For all individuals, variants located on a same read pair were directly phased using
435 physical phasing information. Non-related *D. labrax* individuals were then statistically phased using
436 the reference-based phasing algorithm implemented in Eagle2 (version 2.4) (35). The 22 parents
437 phased with the phasing-by-transmission approach were used to build a European sea bass reference
438 haplotype library (F1 genomes were excluded since their haplotype information was redundant with
439 that of their parents), which was used in Eagle2 to improve statistical phasing. We finally filtered out

440 SNPs that were not phased or not genotyped over all individuals (using --max-missing-count 0 and --
441 phased in VCFtools), to generate a dataset of haplotype-resolved whole-genome sequences from 68
442 unrelated *D. labrax* individuals (14 AT, 31 WME, 11 SEM and 12 NEM), containing 5,074,249 phased
443 SNPs without missing data. The genetic relationships of the newly sequenced genomes with respect to
444 the 16 already available was evaluated with a Principal Component Analysis (Supplementary Figure 2).
445 Although we detected a slight genetic differentiation between North and South eastern Mediterranean
446 samples on the PCA (Supplementary Figure 2), we later determined that they present similar genome-
447 wide average levels of Atlantic ancestry and introgressed tract length (18,148 bp for the South and
448 17,769 bp for the North, Supplementary Figure 5). Therefore, we regrouped these samples together
449 within a single eastern Mediterranean population, similarly to Duranton et al. (2018).

450

451 **Phylogenomic analyses**

452 We used RAxML v.8.2.12 (36) to generate maximum-likelihood trees of Moronids genomes in non-
453 overlapping 50 kb windows (including *Morone saxatilis*, *D. punctatus* and the Atlantic and
454 Mediterranean *D. labrax* lineages). Ancient admixture is expected to generate discordant trees among
455 genomic windows. However, if admixture is ancient, introgressed tracts may be too short to influence
456 the phylogenetic signal in 50 kb windows. Therefore, we did the same analyses using a 2 kb window
457 size to increase the resolution of local genealogies while keeping enough informative sites. In order to
458 account for disparities among species' genome sequence datasets, we used only one individual
459 haplome for each species/lineage for this analysis. The alignment of these four haplomes spanned 52%
460 of the *D. labrax* genome, a fact largely due to the fragmentation of the *M. saxatilis* (SAX) genome that
461 produced discontinuous local alignments to the *D. labrax* reference genome (30). In order to account
462 for this fragmentation, we only analyzed windows with less than 10% missing data in local alignments.
463 We obtained 3,329 and 155,155 trees under the GTRGAMMA model for analyses based on 50 and 2
464 kb windows, respectively. Trees generated in windows of similar size were then superposed using
465 DensiTree v2.2.5 (37) for visualization. In order to provide indications for genome-wide average
466 absolute sequence divergence between all pairs of species and lineages, we calculated d_{xy} with the
467 same individual haplomes used for the RAxML analysis using MVFTools v5.1.2 (38) and averaged
468 distance values calculated in non-overlapping 50kb windows.

469

470 **Tests for foreign introgression within *D. labrax***

471 We tested for admixture between *D. labrax* and another species using three different methods that
472 capture complementary aspects of the data. Since *D. punctatus* is the only closely related species
473 parapatrically distributed with *D. labrax*, we first tested for historical gene flow between these two
474 species. To do so, we used the ABBA-BABA test (19,23) with *M. saxatilis* as the outgroup (O), *D.*

475 *punctatus* as the potential donor species (P3) and the two *D. labrax* lineages as potential recipient
476 populations (P1 and P2). We used the dataset containing 14,579,961 SNPs from *D. punctatus* and
477 unphased *D. labrax* samples, and only kept sites that were available for both *M. saxatilis* and *D.*
478 *punctatus* in genome alignments, representing a total of 9,606,462 SNPs. This allowed testing for
479 different amounts of gene flow between P3 and P2, and P3 and P1, by comparing the number of
480 genealogies of type ((P1,(P2,P3),O) (*i.e.* ABBA genealogies) and ((P2,(P1,P3),O) (*i.e.* BABA genealogies).
481 An excess of shared derived alleles between the donor and one of the two recipient populations (*i.e.*
482 excess of ABBA over BABA genealogies, or vice versa) indicates gene flow from *D. punctatus* to *D.*
483 *labrax* population P2 or P1, respectively. Although the ABBA-BABA test is adequate to detect
484 introgression, the Patterson's *D* statistic that measures the imbalance between the two types of
485 genealogies ($D = \frac{\text{sum}(ABBA) - \text{sum}(BABA)}{\text{sum}(ABBA) + \text{sum}(BABA)}$) is not appropriate to quantify introgression over small
486 genomic windows (39). Therefore, we used the f_D statistics ($f_D = \frac{s(P1,P2,P3,O)}{s(P1,PD,PD,O)}$) to estimate admixture
487 proportion between P2 et P3, where $s = \text{sum}(ABBA - BABA)$ and PD corresponds to the most likely donor
488 population (*i.e.* the population with the higher frequency of the derived allele). In order to test for
489 admixture between *D. punctatus* and different populations of *D. labrax*, we made different tests using
490 successively the Atlantic (AT), eastern (EME combining SEM and NEM individuals), western (WME) or
491 the whole Mediterranean (MED) populations of *D. labrax* populations as P2 or P1. We used scripts
492 from Martin *et al.* (2015) to estimate the number of ABBA and BABA genealogies and the f_D statistics
493 in non-overlapping 50 kb windows along the genome, keeping only windows containing at least 500
494 SNPs.

495 Secondly, we used a method that allows identifying archaic introgressed tracts without using
496 an archaic reference genome for the donor species (40). The main advantage of this method is that it
497 makes no assumption on the identity of the donor species. Basically, it looks for local excesses of
498 private variants in a candidate recipient population by comparison to another non-admixed population
499 (40). In order to test for archaic introgression within the Atlantic *D. labrax* lineage, we identified
500 variants that were not shared with the eastern Mediterranean population, and conversely to test for
501 introgression in the Mediterranean *D. labrax* lineage. We only analyzed the eastern Mediterranean
502 population because the western Mediterranean is more strongly impacted by gene flow from the
503 Atlantic (30,32). We used the phased genomes dataset containing 5,074,249 SNPs, assuming a
504 constant mutation and call rate to run the model in 1000 bp windows along each chromosome. For
505 each window, the probability that an individual haplotype contains an archaic introgressed fragment
506 was estimated to identify introgressed windows with a posterior probability superior to 0.8 (40). We
507 then combined individual profiles of introgressed windows to estimate the fraction of introgressed
508 archaic tracts in each population (F_{archaic}), as the fraction of haplotypes for which a window was

509 identified as introgressed. The inferred fraction of introgressed archaic tracts was finally averaged in
510 non-overlapping 50 kb windows along the genome.

511 Finally, we used the RND_{min} statistics, which is sensitive to rare introgression while being robust
512 to mutation rate variation across the genome (41). The main advantage of this statistic is that, unlike
513 the two former methods, it does not rely on the comparison of two recipient populations that differ in
514 their level of introgression. The RND_{min} corresponds to the ratio of the minimal pairwise distance
515 between haplotypes from the potential donor and recipient populations (d_{min}) over the average
516 divergence of those populations to an outgroup species (d_{out}). If gene flow has occurred genome-wide,
517 then locally elevated RND_{min} values indicate regions where introgression has been limited or absent.
518 We used MVFTools v5.1.2 (38) to measure d_{min} between *D. punctatus* and different population of *D.*
519 *labrax* (AT, EME, WME, MED). For this analysis, we used 4,943,488 SNPs polymorphic sites that were
520 phased within *D. labrax* and non-missing in *D. punctatus*. On one hand, this dataset excludes a large
521 number of variants that are differentially fixed between *D. punctatus* and *D. labrax*, and therefore
522 underestimates the real level of divergence between *D. punctatus* and *D. labrax*. On the other hand,
523 excluding diagnostic SNPs rendered the test more sensitive to the detection of ancient introgression,
524 since the accumulation of divergence after introgression only adds noise to chromosomal variations in
525 RND_{min} . We estimated d_{out} by averaging the divergence measures between *M. saxatilis* and the two
526 *Dicentrarchus* species. All values were averaged in non-overlapping 50 kb windows along the genome.

527

528 **Detection of introgressed tracts between Atlantic and Mediterranean *D. labrax* lineages**

529 In order to test whether ancient introgression has influenced genomic patterns of post-glacial gene
530 flow between Atlantic and Mediterranean *D. labrax* lineages, we mapped Atlantic tracts introgressed
531 into Mediterranean genomes and conversely. Local ancestry inference was performed with
532 Chromopainter v0.04 (42), an HMM-based program that estimates the probability of Atlantic and
533 Mediterranean ancestry for each variable position along each haplome. To do so, it compares a focal
534 haplotype to reference populations composed of non-introgressed Atlantic and Mediterranean
535 haplotypes. Since Mediterranean individuals are introgressed to various extents by Atlantic alleles, we
536 used a pure Mediterranean reference population reconstituted by Duranton *et al.* (2018) with the
537 same model parameters. We then identified the starting and ending position of each introgressed tract
538 within both Atlantic and Mediterranean genetic backgrounds by analyzing the ancestry probability
539 profiles inferred by Chromopainter, following the same methodology as in Duranton *et al.* (2018).
540 Identified tracts in each *D. labrax* population (Supplementary Figure 5) were then combined to
541 estimate the fraction of introgressed tracts (F_{intro}) for each position along the genome, which was finally
542 averaged in non-overlapping 50 kb windows.

543

544 ***Delineation of RI regions between Atlantic and Mediterranean D. labrax lineages***

545 We adapted the HMM approach developed by Hofer *et al.* (2012) to precisely delineate genomic
546 regions involved in RI between Atlantic and Mediterranean *D. labrax* lineages. Genomic regions
547 involved in RI between European sea bass lineages are characterized by elevated genetic
548 differentiation and increased resistance to gene flow (30,32). Therefore, we combined both measures
549 of F_{ST} (43,44) and resistance to introgression measured as the inverse of F_{intro} (28,30). To identify true
550 RI islands in our HMM strategy, we thus used the ratio of F_{ST} over F_{intro} (i.e. the frequency of Atlantic
551 tracts within western Mediterranean *D. labrax* genomes). Our rationale was that these regions should
552 be associated with both high F_{ST} (Supplementary Figure 6A and D) and low F_{intro} values (Supplementary
553 Figure 6B and E) (30), hence elevated F_{ST}/F_{intro} ratio values (Supplementary Figure 6C and F). We used
554 the HMM approach to map RI at two different scales, a SNP-by-SNP (Supplementary Figure 6A-C) and
555 a 50kb window scale, which was more suitable to delineate regions (Supplementary Figure 6D-F). We
556 used VCFtools v0.1.15 (34) to estimate F_{ST} between the Atlantic and the western Mediterranean *D.*
557 *labrax* lineage for each SNPs and every non-overlapping 50kb window along the genome. The HMM
558 was designed with three different states corresponding to low (i.e. neutral genomic regions),
559 intermediate (i.e. regions experiencing linked selection) and high F_{ST}/F_{intro} ratio values (i.e. regions
560 involved in RI). The most likely state of each SNP/window was inferred by running the HMM algorithm
561 chromosome by chromosome. Finally, we controlled for false discovery rate and retained only
562 SNPs/windows with an FDR-corrected p-value inferior to 0.001 (43).

563

564 ***Estimation of the time since foreign introgression within D. labrax***

565 We used two different approaches to estimate the time since foreign introgression within *D. labrax*.
566 First, we relied on the fact that the length of introgressed tracts is informative of the time elapsed
567 since introgression. Recombination progressively shortens migrant tracts across generations following
568 introgression into a new genetic background (45,46). Since we found a good correspondence between
569 the inferred fraction of introgressed archaic tracts ($F_{intro-archaic}$) and f_D values (see results) using *D.*
570 *punctatus* as a donor species, we used the length of archaic haplotypes that were identified with the
571 method of Skov *et al.* (2018). Only archaic tracts found in Atlantic genomes within windows involved
572 in RI between Atlantic and Mediterranean *D. labrax* lineages were considered, corresponding to 1310
573 windows of 50 kb. This choice was justified because archaic tract detection relies on a signal of
574 differential introgression between two populations. Therefore, archaic tracts can be correctly
575 identified and delimited only if they are present in one lineage (e.g. the Atlantic) but absent in the
576 other (e.g. the Mediterranean), which was only the case in RI islands between Atlantic and
577 Mediterranean *D. labrax* lineages (see results).

578 Under simple assumptions, there is an analytical expectation for the average length of
579 introgressed tracts (\bar{L}) as a function of the number of generations since introgression (t), the local
580 recombination rate (r in Morgans per bp) and the proportion of admixture (f), which takes the form \bar{L}
581 $= [(1 - f) r (t - 1)]^{-1}$ (26). We used this equation to estimate the age of admixture between *D.*
582 *punctatus* and the Atlantic lineage of *D. labrax* ($t_{\text{labrax-punctatus}}$), as well as between the two lineages of
583 *D. labrax* ($t_{\text{Atlantic-Mediterranean}}$). For each estimation, we used the average value of the retained windows.
584 Hence, for $t_{\text{labrax-punctatus}}$: $f = 0.096$, $r = 3.693e^{-8}$ M/bp (32) and $\bar{L} = 5,513$ bp, and for $t_{\text{Atlantic-Mediterranean}}$: f
585 $= 0.341$, $r = 3.23e^{-8}$ M/bp, and $\bar{L} = 52,026$ bp. Since we only considered a relatively small fraction of the
586 genome to call archaic tracts, we could not obtain precise estimations of those parameters. Therefore,
587 we estimated the age of contact between *D. punctatus* and *D. labrax* by reference to the age of the
588 post-glacial secondary contact between Atlantic and Mediterranean lineages of *D. labrax*, which has
589 been more precisely estimated to 2,300 generations using a larger fraction of the genome (30,32).

590 Secondly, we transformed the estimated transition parameter values of the HMM model used
591 to detect archaic introgressed tracts using $p \approx T_{\text{admixture}} \cdot 2 \cdot r \cdot L \cdot a$ (40). In this equation, p is the
592 probability of transition from the *D. labrax* to the archaic ancestry state, $T_{\text{admixture}}$ represents the
593 admixture time in generations, r the recombination rate in Morgan per bp, a the admixture proportion
594 and L the size of the window (here $L = 1000$ bp). Parameter p was estimated separately for each
595 chromosome by averaging over the values estimated per individual haplome. We finally estimated
596 $T_{\text{admixture}}$ chromosome by chromosome using the average recombination rate and the fraction of archaic
597 introgressed tracts of each chromosome (Supplementary Table 2). The time in generations was
598 converted into years using a generation time of 5 years (32). We then obtained a distribution for $T_{\text{admixture}}$
599 across the 24 chromosomes, from which we identified the maximum and its 90% confidence interval
600 by bootstrapping the distribution 10,000 times.

601

602 **Characterizing foreign ancestry tracts within *D. labrax***

603 We used Spearman's correlation test to evaluate relationships among $F_{\text{intro-archaic}}$, f_D , d_{XY} and RND_{min}
604 statistics that relate to a series of predictive hypotheses. More specifically, if *D. punctatus* has anciently
605 contributed to *D. labrax* in the Atlantic, the local abundance of archaic tracts inferred within Atlantic
606 *D. labrax* genomes (F_{archaic}) should be positively correlated to f_D . Moreover, if the abundance of archaic
607 tracts within Atlantic *D. labrax* explains the presence of anciently diverged alleles between Atlantic and
608 Mediterranean sea bass lineages, d_{XY} should increase with the amount of ancient admixture. Finally, if
609 regions involved in RI between Atlantic and Mediterranean sea bass lineages harbor reduced
610 frequencies of *D. punctatus* derived tracts in the Mediterranean, a positive correlation is expected
611 between RND_{min} measured between *D. punctatus* and Mediterranean *D. labrax* and ancient admixture
612 from *D. punctatus* within the Atlantic.

613 We then focused on SNP-level statistics to specifically address the frequency distributions of
614 derived mutations from *D. punctatus* within *D. labrax* genomes, separately in the Atlantic and
615 Mediterranean lineages. Since anciently introgressed alleles most likely originated from *D. punctatus*
616 (see results), we used *D. labrax* polymorphic sites for which *M. saxatilis* harbors the ancestral and *D.*
617 *punctatus* the derived state (i.e. ABBA-BABA informative sites) to characterize ancient introgression.
618 For each of these SNPs, we measured the frequency of the *D. punctatus* derived allele separately in
619 the Atlantic and Mediterranean *D. labrax* populations using VCFtools. We then separated SNPs
620 associated to RI islands from those that were not associated to RI islands in the SNP-based HMM
621 analysis to represent the site frequency spectrum of each *D. labrax* lineage, conditioned on *D.*
622 *punctatus* being derived (CSFS). Finally, two conditioned joint site frequency spectra (CJSFS) were
623 generated (i.e. for RI and non-RI SNPs) to represent the bi-dimensional SFS between Atlantic and
624 Mediterranean *D. labrax* lineages, conditioning on sites that have the derived allele in *D. punctatus*.
625 These analyses aimed at distinguishing two hypotheses with respect to the mechanisms underlying
626 differential introgression of *D. punctatus* derived mutations in RI islands between Atlantic and
627 Mediterranean *D. labrax*. Our first hypothesis was that anciently introgressed alleles are not directly
628 involved in RI but simply maintained at different frequencies because genetic barriers between *D.*
629 *labrax* lineages (i.e. unrelated to the history of ancient admixture) have impeded their post-glacial
630 rehomogenization. In this case, we expected no excess of high-frequency *D. punctatus* derived
631 mutations in RI islands compared to non-RI regions. Alternatively, under the hypothesis that anciently
632 introgressed alleles are associated with reproductive isolation in sea bass, an excess of *D. punctatus*
633 derived mutations almost fixed within RI islands in the Atlantic but nearly absent in the Mediterranean
634 was expected compared to the alternate configuration (i.e. almost fixed in the Mediterranean and
635 nearly absent in the Atlantic).

636

637

638

Acknowledgement

639 This work was co-funded by the GeneSea project (n° R FEA 4700 16 FA 100 0005) by the French
640 Government and the European Union (EMFF, European Maritime and Fisheries Fund) at the "Appels à
641 projets Innovants" managed by the FranceAgrimer Office and the ANR grant CoGeDiv (ANR-17-CE02-
642 0006-01 to P.-A.G). This work was performed in collaboration with the GeT core facility, Toulouse,
643 France (<http://get.genotoul.fr>), and was supported by France Génomique National infrastructure,
644 funded as part of "Investissement d'avenir" program managed by Agence Nationale pour la Recherche
645 (contract ANR-10-INBS-09). We also thank Ifremer's experimental aquaculture platform for the
646 breeding and the rearing of the hybrid populations

References

1. Coyne JA, Orr AH. Speciation. Sinauer Associates. Massachusetts U.S.A.: Sunderland MA; 2004.
2. Presgraves DC. The molecular evolutionary basis of species formation. *Nature Reviews Genetics*. mars 2010;11(3):175-80.
3. Wolf Jochen B. W., Lindell Johan, Backström Niclas. Speciation genetics: current status and evolving approaches. *Philosophical Transactions of the Royal Society B: Biological Sciences*. 12 juin 2010;365(1547):1717-33.
4. Feder JL, Egan SP, Nosil P. The genomics of speciation-with-gene-flow. *Trends in Genetics*. 1 juill 2012;28(7):342-50.
5. Seehausen O, Butlin RK, Keller I, Wagner CE, Boughman JW, Hohenlohe PA, et al. Genomics and the origin of species. *Nat Rev Genet*. mars 2014;15(3):176-92.
6. Harrison RG, Larson EL. Heterogeneous genome divergence, differential introgression, and the origin and structure of hybrid zones. *Mol Ecol*. 1 juin 2016;25(11):2454-66.
7. Wolf JBW, Ellegren H. Making sense of genomic islands of differentiation in light of speciation. *Nat Rev Genet*. 14 nov 2016;18:87-100.
8. Ravinet M, Faria R, Butlin RK, Galindo J, Bierne N, Rafajlović M, et al. Interpreting the genomic landscape of speciation: a road map for finding barriers to gene flow. *J Evol Biol*. 1 août 2017;30(8):1450-77.
9. Fuller ZL, Leonard CJ, Young RE, Schaeffer SW, Phadnis N. Ancestral polymorphisms explain the role of chromosomal inversions in speciation. *PLOS Genetics*. 30 juill 2018;14(7):e1007526.
10. Colosimo PF, Hosemann KE, Balabhadra S, Villarreal G, Dickson M, Grimwood J, et al. Widespread Parallel Evolution in Sticklebacks by Repeated Fixation of Ectodysplasin Alleles. *Science*. 25 mars 2005;307(5717):1928-33.
11. Nelson TC, Cresko WA. Ancient genomic variation underlies repeated ecological adaptation in young stickleback populations. *Evolution Letters*. 2018;2(1):9-21.
12. Marques DA, Meier JI, Seehausen O. A Combinatorial View on Speciation and Adaptive Radiation. *Trends in Ecology & Evolution [Internet]*. 15 mars 2019 [cité 10 avr 2019]; Disponible sur: <http://www.sciencedirect.com/science/article/pii/S0169534719300552>
13. Han F, Lamichhaney S, Grant BR, Grant PR, Andersson L, Webster MT. Gene flow, ancient polymorphism, and ecological adaptation shape the genomic landscape of divergence among Darwin's finches. *Genome Res [Internet]*. 25 avr 2017 [cité 10 janv 2019]; Disponible sur: <http://genome.cshlp.org/content/early/2017/04/25/gr.212522.116>
14. Guerrero RF, Hahn MW. Speciation as a Sieve for Ancestral Polymorphism. *Mol Ecol [Internet]*. 2017 [cité 11 août 2017]; Disponible sur: <http://onlinelibrary.wiley.com/doi/10.1111/mec.14290/abstract>

15. Slatkin M, Pollack JL. Subdivision in an Ancestral Species Creates Asymmetry in Gene Trees. *Mol Biol Evol.* 1 oct 2008;25(10):2241-6.
16. Charlesworth D. Balancing Selection and Its Effects on Sequences in Nearby Genome Regions. *PLOS Genetics.* 28 avr 2006;2(4):e64.
17. Abbott R, Albach D, Ansell S, Arntzen JW, Baird SJE, Bierne N, et al. Hybridization and speciation. *J Evol Biol.* 1 févr 2013;26(2):229-46.
18. Payseur BA, Rieseberg LH. A genomic perspective on hybridization and speciation. *Mol Ecol.* 1 juin 2016;25(11):2337-60.
19. Green RE, Krause J, Briggs AW, Maricic T, Stenzel U, Kircher M, et al. A Draft Sequence of the Neandertal Genome. *Science.* 7 mai 2010;328(5979):710-22.
20. Meyer M, Kircher M, Gansauge M-T, Li H, Racimo F, Mallick S, et al. A High-Coverage Genome Sequence from an Archaic Denisovan Individual. *Science.* 12 oct 2012;338(6104):222-6.
21. Pääbo S. The diverse origins of the human gene pool. *Nature Reviews Genetics.* 18 mai 2015;16:313-4.
22. Barlow A, Cahill JA, Hartmann S, Theunert C, Xenikoudakis G, Fortes GG, et al. Partial genomic survival of cave bears in living brown bears. *Nature Ecology & Evolution.* oct 2018;2(10):1563-70.
23. Durand EY, Patterson N, Reich D, Slatkin M. Testing for Ancient Admixture between Closely Related Populations. *Mol Biol Evol.* 1 août 2011;28(8):2239-52.
24. Eriksson A, Manica A. Effect of ancient population structure on the degree of polymorphism shared between modern human populations and ancient hominins. *Proc Natl Acad Sci U S A.* 28 août 2012;109(35):13956-60.
25. Welch JJ, Jiggins CD. Standing and flowing: the complex origins of adaptive variation. *Molecular Ecology.* 2014;23(16):3935-7.
26. Racimo F, Sankararaman S, Nielsen R, Huerta-Sánchez E. Evidence for archaic adaptive introgression in humans. *Nat Rev Genet.* juin 2015;16(6):359-71.
27. Theunert C, Slatkin M. Distinguishing Recent Admixture from Ancestral Population Structure. *Genome Biol Evol.* 1 mars 2017;9(3):427-37.
28. Cruickshank TE, Hahn MW. Reanalysis suggests that genomic islands of speciation are due to reduced diversity, not reduced gene flow. *Mol Ecol.* 1 juill 2014;23(13):3133-57.
29. Schumer M, Xu C, Powell DL, Durvasula A, Skov L, Holland C, et al. Natural selection interacts with recombination to shape the evolution of hybrid genomes. *Science.* 19 avr 2018;eaar3684.
30. Durantou M, Allal F, Fraïsse C, Bierne N, Bonhomme F, Gagnaire P-A. The origin and remolding of genomic islands of differentiation in the European sea bass. *Nature Communications.* 28 juin 2018;9(1):2518.

31. Lemaire C, Versini J-J, Bonhomme F. Maintenance of genetic differentiation across a transition zone in the sea: discordance between nuclear and cytoplasmic markers. *Journal of Evolutionary Biology*. 1 janv 2005;18(1):70-80.
32. Tine M, Kuhl H, Gagnaire P-A, Louro B, Desmarais E, Martins RS, et al. European sea bass genome and its variation provide insights into adaptation to euryhalinity and speciation. *Nature Communications*. 2014;5:5770.
33. Li H. Aligning sequence reads, clone sequences and assembly contigs with BWA-MEM. arXiv: preprint [Internet]. 16 mars 2013 [cité 27 avr 2017]; Disponible sur: <http://arxiv.org/abs/1303.3997>
34. Danecek P, Auton A, Abecasis G, Albers CA, Banks E, DePristo MA, et al. The variant call format and VCFtools. *Bioinformatics*. 8 janv 2011;27(15):2156-8.
35. Loh P-R, Danecek P, Palamara PF, Fuchsberger C, Reshef YA, Finucane HK, et al. Reference-based phasing using the Haplotype Reference Consortium panel. *Nature Genetics*. nov 2016;48(11):1443-8.
36. Stamatakis A. RAxML version 8: a tool for phylogenetic analysis and post-analysis of large phylogenies. *Bioinformatics*. 1 mai 2014;30(9):1312-3.
37. Bouckaert R, Heled J. DensiTree 2: Seeing Trees Through the Forest. *bioRxiv*. 8 déc 2014;012401.
38. Pease J, Rosenzweig B. Encoding Data Using Biological Principles: the Multisample Variant Format for Phylogenomics and Population Genomics. *IEEE/ACM Transactions on Computational Biology and Bioinformatics*. 2015;PP(99):1-1.
39. Martin SH, Davey JW, Jiggins CD. Evaluating the Use of ABBA–BABA Statistics to Locate Introgressed Loci. *Mol Biol Evol*. 1 janv 2015;32(1):244-57.
40. Skov L, Hui R, Shchur V, Hobolth A, Scally A, Schierup MH, et al. Detecting archaic introgression using an unadmixed outgroup. *PLOS Genetics*. 18 sept 2018;14(9):e1007641.
41. Rosenzweig BK, Pease JB, Besansky NJ, Hahn MW. Powerful methods for detecting introgressed regions from population genomic data. *Mol Ecol*. 1 mars 2016;2387-97.
42. Lawson DJ, Hellenthal G, Myers S, Falush D. Inference of Population Structure using Dense Haplotype Data. *PLOS Genet* [Internet]. 26 janv 2012 [cité 4 avr 2016];8(1). Disponible sur: <http://journals.plos.org/plosgenetics/article?id=10.1371/journal.pgen.1002453>
43. Hofer T, Foll M, Excoffier L. Evolutionary forces shaping genomic islands of population differentiation in humans. *BMC Genomics*. 22 mars 2012;13:107.
44. Marques DA, Lucek K, Meier JI, Mwaiko S, Wagner CE, Excoffier L, et al. Genomics of Rapid Incipient Speciation in Sympatric Threespine Stickleback. *PLOS Genetics* [Internet]. 29 févr 2016 [cité 11 mai 2017];12(2). Disponible sur: <http://journals.plos.org/plosgenetics/article?id=10.1371/journal.pgen.1005887>
45. Pool JE, Nielsen R. Inference of Historical Changes in Migration Rate From the Lengths of Migrant Tracts. *Genetics*. 1 févr 2009;181(2):711-9.

46. Liang M, Nielsen R. The Lengths of Admixture Tracts. *Genetics*. 1 juill 2014;197(3):953-67.
47. Meier JI, Marques DA, Mwaiko S, Wagner CE, Excoffier L, Seehausen O. Ancient hybridization fuels rapid cichlid fish adaptive radiations. *Nature Communications*. 10 févr 2017;8:14363.
48. Ky C-L, Vergnet A, Molinari N, Fauvel C, Bonhomme F. Fitness of early life stages in F1 interspecific hybrids between *Dicentrarchus labrax* and *D. punctatus*. *Aquat Living Resour*. 1 janv 2012;25(1):67-75.
49. Sankararaman S, Mallick S, Patterson N, Reich D. The Combined Landscape of Denisovan and Neanderthal Ancestry in Present-Day Humans. *Current Biology*. 9 mai 2016;26(9):1241-7.
50. Harris K, Nielsen R. The Genetic Cost of Neanderthal Introgression. *Genetics*. 1 juin 2016;203(2):881-91.
51. Juric I, Aeschbacher S, Coop G. The Strength of Selection against Neanderthal Introgression. *PLOS Genetics*. 8 nov 2016;12(11):e1006340.
52. Gopalakrishnan S, Sinding M-HS, Ramos-Madrugal J, Niemann J, Castruita JAS, Vieira FG, et al. Interspecific Gene Flow Shaped the Evolution of the Genus *Canis*. *Current Biology [Internet]*. 18 oct 2018 [cité 24 oct 2018];0(0). Disponible sur: [https://www.cell.com/current-biology/abstract/S0960-9822\(18\)31125-4](https://www.cell.com/current-biology/abstract/S0960-9822(18)31125-4)
53. Snyder CW. Evolution of global temperature over the past two million years. *Nature*. 13 oct 2016;538(7624):226-8.
54. Hewitt G. The genetic legacy of the Quaternary ice ages. *Nature*. 22 juin 2000;405(6789):907-13.
55. Maggs CA, Castilho R, Foltz D, Henzler C, Jolly MT, Kelly J, et al. Evaluating Signatures of Glacial Refugia for North Atlantic Benthic Marine Taxa. *Ecology*. 2008;89(sp11):S108-22.
56. Schumer M, Rosenthal GG, Andolfatto P. How Common Is Homoploid Hybrid Speciation? *Evolution*. 2014;68(6):1553-60.
57. Schumer M, Rosenthal GG, Andolfatto P. What do we mean when we talk about hybrid speciation? *Heredity*. avr 2018;120(4):379.
58. Racimo F, Marnetto D, Huerta-Sánchez E. Signatures of Archaic Adaptive Introgression in Present-Day Human Populations. *Mol Biol Evol*. 1 févr 2017;34(2):296-317.
59. Huerta-Sánchez E, Jin X, Asan, Bianba Z, Peter BM, Vinckenbosch N, et al. Altitude adaptation in Tibetans caused by introgression of Denisovan-like DNA. *Nature*. 14 août 2014;512(7513):194-7.
60. Dasmahapatra KK, Walters JR, Briscoe AD, Davey JW, Whibley A, Nadeau NJ, et al. Butterfly genome reveals promiscuous exchange of mimicry adaptations among species. *Nature*. 5 juill 2012;487(7405):94-8.
61. Jones MR, Mills LS, Alves PC, Callahan CM, Alves JM, Lafferty DJR, et al. Adaptive introgression underlies polymorphic seasonal camouflage in snowshoe hares. *Science*. 22 juin 2018;360(6395):1355-8.

62. Martin SH, Jiggins CD. Interpreting the genomic landscape of introgression. *Current Opinion in Genetics & Development*. déc 2017;47:69-74.
63. Hedrick PW. Adaptive introgression in animals: examples and comparison to new mutation and standing variation as sources of adaptive variation. *Molecular Ecology*. 2013;22(18):4606-18.
64. Fraïsse C, Roux C, Welch JJ, Bierne N. Gene-Flow in a Mosaic Hybrid Zone: Is Local Introgression Adaptive? *Genetics*. 1 juill 2014;197(3):939-51.
65. Barton NH. Does hybridization influence speciation? *Journal of Evolutionary Biology*. 2013;26(2):267-9.
66. Whitlock MC, Ingvarsson PÅK, Hatfield T. Local drift load and the heterosis of interconnected populations. *Heredity*. 2000;84(4):452-7.
67. Bierne N, Lenormand T, Bonhomme F, David P. Deleterious mutations in a hybrid zone: can mutational load decrease the barrier to gene flow? *Genetics Research*. déc 2002;80(3):197-204.
68. Kim BY, Huber CD, Lohmueller KE. Deleterious variation shapes the genomic landscape of introgression. *PLOS Genetics*. 22 oct 2018;14(10):e1007741.
69. Shpak M. The Role of Deleterious Mutations in Allopatric Speciation. *Evolution*. 2005;59(7):1389-99.
70. Kimura M. The role of compensatory neutral mutations in molecular evolution. *J Genet*. 1 juill 1985;64(1):7.
71. Schumer M, Cui R, Rosenthal GG, Andolfatto P. Reproductive Isolation of Hybrid Populations Driven by Genetic Incompatibilities. *PLOS Genetics*. 13 mars 2015;11(3):e1005041.
72. Blanckaert A, Bank C. In search of the Goldilocks zone for hybrid speciation. *PLOS Genetics*. 7 sept 2018;14(9):e1007613.
73. Dobzhansky T grigorovitch. *Genetics and the origin of species*. Columbia university press. 1937.
74. Runemark A, Trier CN, Eroukhmanoff F, Hermansen JS, Matschiner M, Ravinet M, et al. Variation and constraints in hybrid genome formation. *Nature Ecology & Evolution*. mars 2018;2(3):549.
75. Eberlein C, Hénault M, Fijarczyk A, Charron G, Bouvier M, Kohn LM, et al. Hybridization is a recurrent evolutionary stimulus in wild yeast speciation. *Nature Communications*. 25 févr 2019;10(1):923.

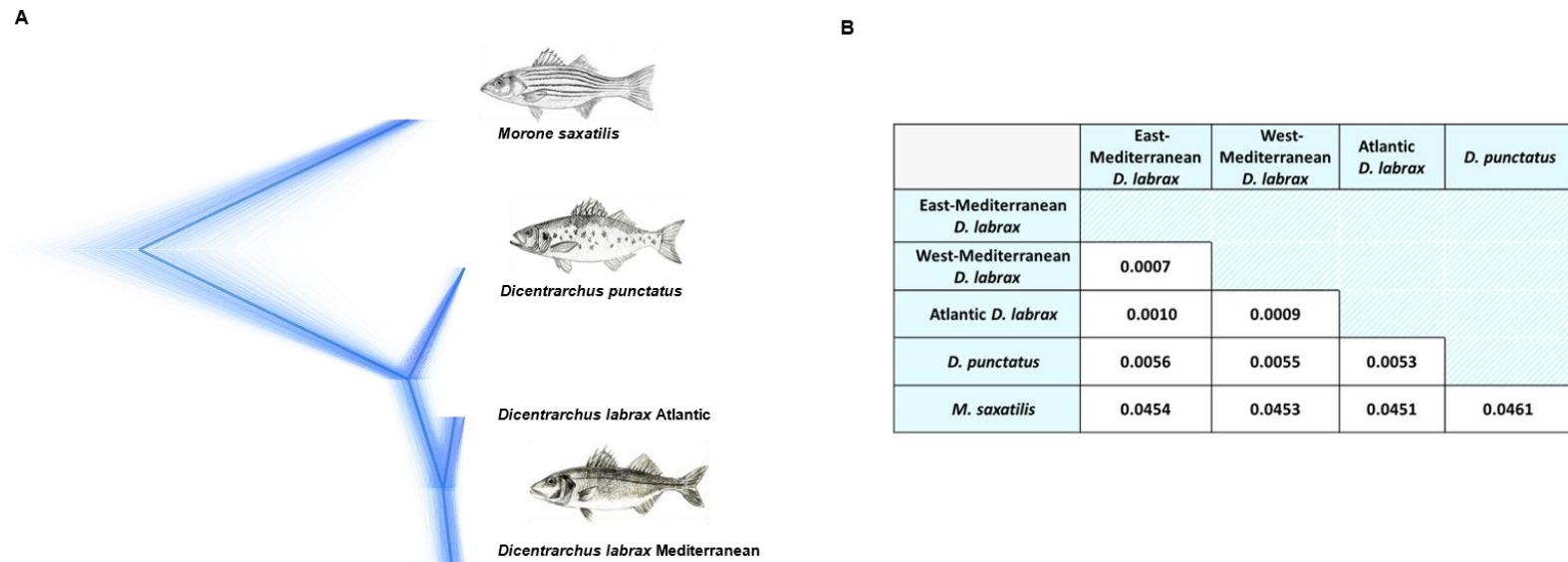


Figure 1 - **Phylogenetic relationships between *D. labrax* lineages, *D. punctatus* and the outgroup species *M. saxatilis*.** **A.** Concordance of 3,329 maximum-likelihood trees reconstructed in non-overlapping 50 kb windows along the genome (thick lines) and superimposed to the consensus species tree (bold line) using DensiTree v2.2.5 (bouckaert and heled 2014). Only one haplome from each species/lineage was used for tree reconstruction. Discordant trees that disproportionately grouped the Atlantic *D. labrax* lineage with *D. punctatus* were observed at a more local scale using 2 kb windows (Supplementary Figure 3). **B.** Genome-wide average pairwise sequence divergence between species/lineages measured by d_{xy} using the same individual haplotypes as for the phylogenetic relationships.

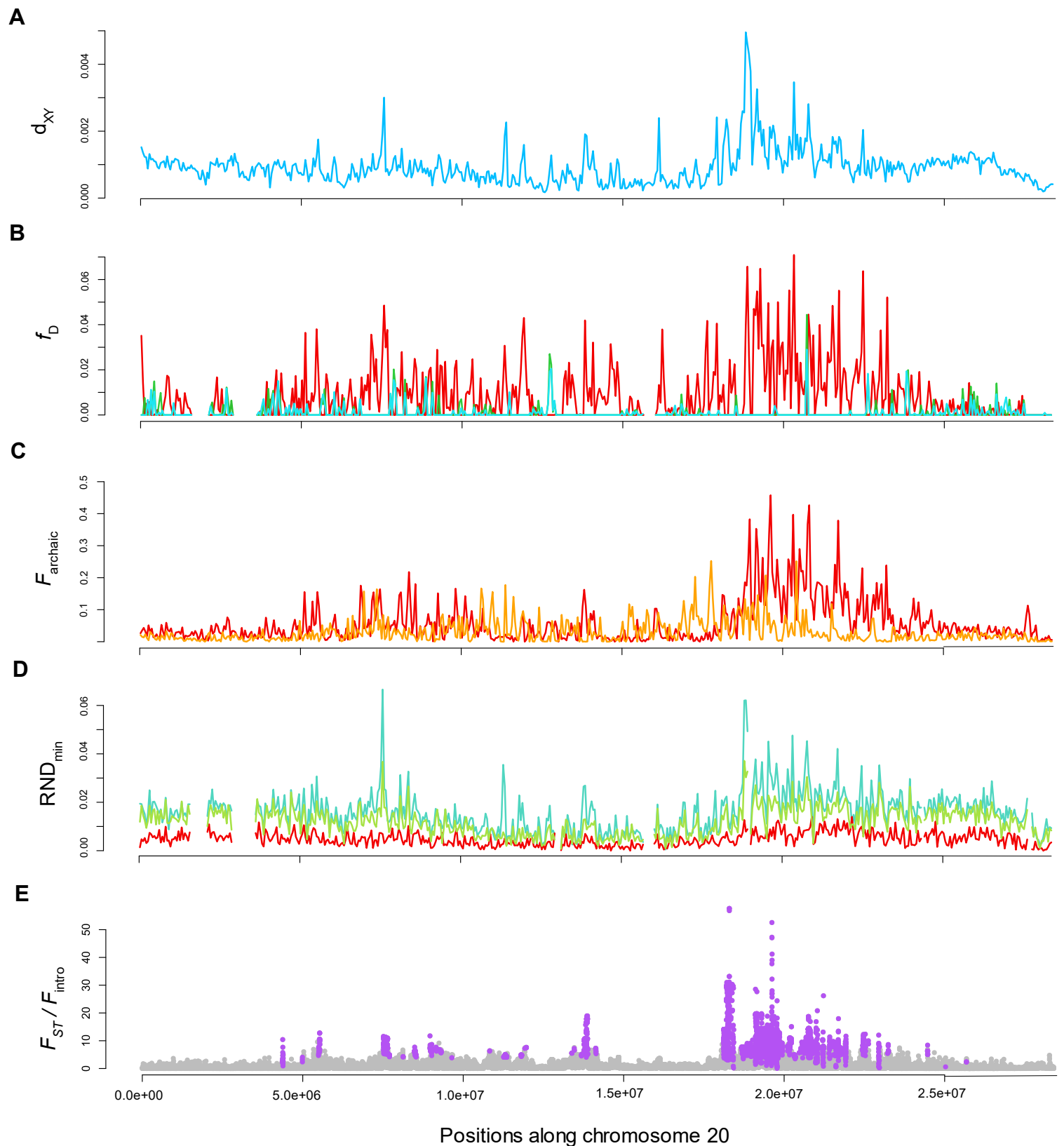


Figure 2 – **Divergence and introgression statistics measured in non-overlapping 50 kb windows along chromosome 20.** **A.** d_{xy} measured between the Atlantic and Mediterranean (including eastern and western population) *D. labrax* lineages. **B.** f_D statistics measured using (((MED, AT), PUN), SAX) in red, (((AT, WEM), PUN), SAX) in green, and (((ATL, SEM), PUN), SAX) in blue. **C.** Fraction of archaic introgressed tracts (F_{archaic}) inferred in the eastern Mediterranean and Atlantic populations of *D. labrax*. **D.** RND_{min} measured between *D. punctatus* and *D. labrax* Atlantic (red), western (green) and eastern (blue) Mediterranean populations. **E.** F_{ST} between the Atlantic and western Mediterranean population of *D. labrax* divided by the fraction of Atlantic tracts introgressed into the western Mediterranean genomes for each SNP along the chromosome. Purple points show SNPs with significant associations to reproductive isolation after applying FDR correction to the probabilities determined with the HMM approach.

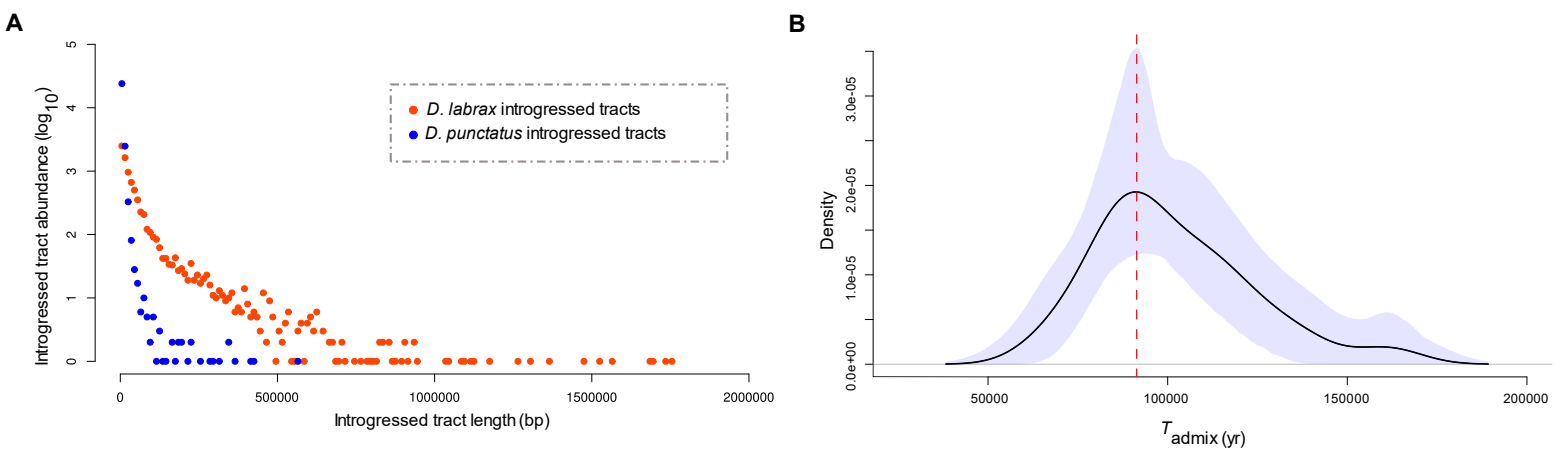


Figure 3 – **Estimation of the time since admixture between *D. punctatus* and Atlantic *D. labrax*.** **A.** Length distributions of *D. punctatus* tracts introgressed into Atlantic *D. labrax* genomes (blue) and Atlantic *D. labrax* tracts introgressed into western Mediterranean *D. labrax* genomes (orange). Both distributions were generated using similar sequence lengths (totalizing 65.6 Mb) along the genomes of 14 Atlantic and 14 Mediterranean individuals, so that tract abundances can be compared. **B.** Distribution of estimated time since admixture between *D. punctatus* and *D. labrax* (T_{admix}) obtained from estimated transition parameter values of the HMM model over the 24 chromosomes. The maximum of the distribution is represented by the vertical red dashed line and the blue shape represents the 95% credibility envelope of the distribution obtained using 10,000 bootstrap resampling.

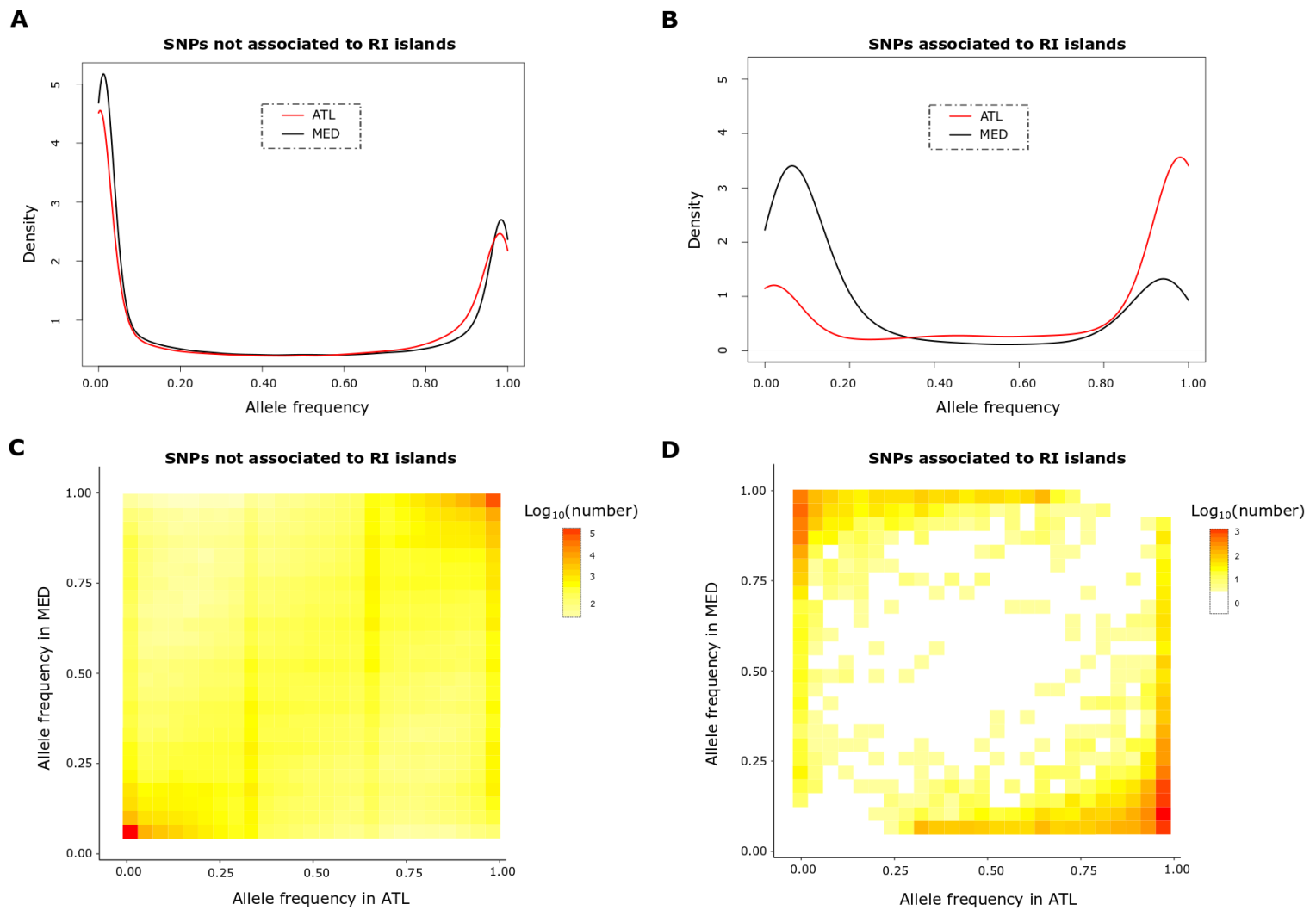


Figure 4 – **One and two-dimensional Site Frequency Spectra of *D. punctatus* derived alleles segregating in *D. labrax*.** **A.** Conditional Site Frequency Spectra (CSFS) of *D. punctatus* derived alleles in AT (red) and MED (black) *D. labrax* lineages for categories of SNPs that are either not associated, or **(B)** associated to RI islands identified between the two *D. labrax* lineages. **C.** Conditional Joint Site Frequency Spectra (CJSFS) of derived *D. punctatus* alleles between MED (54 individuals) and AT (14 individuals) lineages based of 618,842 SNPs not involved in RI, and **(D)** 7,372 SNPs involved in RI.

Supporting Information Legends

Supplementary Table 1 – Summary statistics of sequencing and mapping data for each individual. Individuals whose name is in bold are those involved in crossing.

Supplementary Figure 1 - Depth of coverage per individual. Median (dark gray), first (light gray) and third (black) quartile of the depth of coverage for the 10 Atlantic males (AT), the 23 individuals from the western Mediterranean sea (14 females (F) and 9 males (WM/WME)), the 19 individuals from the eastern Mediterranean sea (9 males from the south (SEM) and 9 males from the north (NEM)), the 7 hybrids (F1) and the *D. punctatus* individual (Punc).

Supplementary Figure 2 - Principal Component Analysis of the European sea bass population genetic structure. The analysis was performed on the 52 newly sequenced genomes (colored circles) and the 16 from a previous data set (1) (gray circles with colorful outline). We used the R package *adegenet* (2) on 91,073 SNPs with a minor allele frequency > 0.4. Individuals originated from four different geographic locations the Atlantic ocean (red, AT), the west (orange, WME), the north-east (dark yellow, NEM) and the south east (light yellow, SEM) of the Mediterranean sea. The first PCA axis explains 39.76% of the total inertia and distinguish the Atlantic and Mediterranean populations while the second PCA axis explains 6.55% of the total inertia and reveals a structure within the Mediterranean population.

Supplementary Figure 3 –Consensus trees of the 155,155 Maximum-likelihood trees inferred in 2kb windows along the genome between *M. saxatilis*, *D. punctatus* and Atlantic and Mediterranean *D. labrax* lineages. There were four different topologies, the most frequent representing the species tree; 94.5% (blue), the second one grouping the Atlantic lineage with *D. punctatus*; 2.87 % (orange), a third one grouping *D. punctatus* with the Mediterranean lineage; 1.68 % (green) and a last one with unresolved relationship between *D. labrax* lineages and *D. punctatus*; 0.05% (not showed).

Supplementary Figure 4 – Statistics measured in non-overlapping 50 kb windows along the genome. A. dXY measured between the Atlantic and Mediterranean (including eastern and western population) *D. labrax* lineage B. fD statistic measured using in red (((MED, AT), PUN), SAX), in green (((AT, WEST), PUN), SAX) and in blue (((AT, EAST), PUN), SAX). C. Fraction of archaic introgressed tracts (Farchaic) in the eastern Mediterranean and Atlantic population of *D. labrax*. D. RNDmin measured between *D. punctatus* and *D. labrax* Atlantic (red), western (green) and eastern (blue) Mediterranean populations. E. Ratio of FST and Fintro used to run the HMM approaches on 50 kb windows that rely on 3 states 1 (light grey), 2 (medium grey) and 3 (dark grey). Red points passed the control for false discovery. We defined island of reproductive isolation as continuous regions containing only red and dark grey points (red boxes). F. Ratio of FST and Fintro used to run the HMM approaches on SNPs, purple points are SNPs identified as involved in reproductive isolation that passed the control for false discovery.

Supplementary Figure 5 – Introgressed tract length distributions. Length distributions of Mediterranean tracts introgressed into the Atlantic population (red) and of Atlantic tracts introgressed into the western (orange), north-eastern (dark yellow) and south-eastern (light yellow) Mediterranean populations. Distributions were generated over the whole genome using 11 individuals per population.

Supplementary Figure 6 – Data and results for the SNPs and 50kb window based HMM approach to identify regions involved in reproductive isolation between the two lineage of *D. labrax* along chromosome 7. A. F_{ST} measured between the Atlantic and western Mediterranean population of *D. labrax* for each SNPs and in every non-overlapping 50 kb windows (D). B. Fraction of Atlantic tracts introgressed in western Mediterranean genomes (Fintro) for each SNPs and in every non-overlapping 50 kb windows (E). C. Statistic analyzed by the HMM approaches (F_{ST} divided by Fintro) for each SNPs and every 50 kb non-overlapping window (F). Ratio of F_{ST} and Fintro used to run the HMM approaches that rely on 3 states that identify; neutral genomic regions (state 1, light grey), genomic regions under linked selection (state 2, medium grey) and genomic regions involved in reproductive isolation (state3, dark grey). Red points are those that passed the control for false discovery. For the window approach we defined island of RI as continuous regions containing only red and dark grey points (red boxes).

Supplementary Figure 7 – Distributions and joint allele-frequency spectrums of derived *D. punctatus* alleles present in *D. labrax*. Distribution of *D. punctatus* derived alleles frequency in AT (red) and WEST (black) (A) or East (D) *D. labrax* individuals for loci involved (solid line) or not (dashed lines) in reproductive isolation between the two *D. labrax* lineages. B. Joint allele-frequency spectrum of derived *D. punctatus* allele for the WEST (31 individuals) and AT (14 individuals) populations for 594,797 SNPs not involved and 7,372 SNPs involved (C) in reproductive isolation. E. Joint allele-frequency spectrum of derived *D. punctatus* allele for the EAST (23 individuals) and AT (14 individuals) populations for 594,454 SNPs not involved and 7,366 SNPs involved (C) in reproductive isolation.

Supplementary Table 2 – values used to estimate Tadmix for each chromosome.